Detrimental Effects of Natural Vertical Head Gradients on Chemical and Water Level Measurements in Observation Wells: Identificaiton and Control

by

G. P. Flach

Westinghouse Savannah River Company
Savannah River Site
Aiken, South Carolina 29808

A. Elci
Clemson University
SC USA

F. J. Molz
Clemson University
SC USA

A document prepared for JOURNAL OF HYDROLOGY at , , from - .

DOE Contract No. **DE-AC09-96SR18500**

This document was prepared in conjunction with work accomplished under Contract No. DE-AC09-96SR18500 with the U. S. Department of Energy.

WSRC-MS-2002-00436 final

Detrimental Effects of Natural Vertical Head Gradients on Chemical and Water Level Measurements in Observation Wells: Identification and Control

by

Alper Elçi [a], Gregory P. Flach [b], and Fred J. Molz [a,*]

[a] Environmental Engineering & Science, Clemson University, 342 Computer Ct., Anderson, SC 29625, USA

[b] Savannah River Technology Center, Aiken, SC 29808, USA

[*] Corresponding author, Tel: (864) 656-1003, Fax: (864) 656-0672, E-mail: fredi@clemson.edu

Abstract

It is well known that vertical head gradients exist in natural aquifer systems, and borehole flowmeter data have shown that such gradients commonly set up spontaneous vertical flows in monitoring wells, often called ambient flows. What has not been fully appreciated until recently is the serious detrimental effects such flows can have on solute concentration (Elci et al., 2001) and hydraulic head measurements in monitoring wells. This communication explores the possibilities of diminishing ambient flows by increasing the hydraulic resistance to vertical flow within monitoring wells and limiting the penetration of such wells. Analyzed also are the surprising effects that vertical gradients may have on the equilibrium water level in a monitoring well. Results are based on collected data, numerical flow simulations, and hydraulic analysis in the near-well vicinity. Raising wellbore hydraulic resistance is of increasing importance and impact in thicker aquifers with higher horizontal hydraulic conductivities (K_h). A systematic analysis of screen penetration revealed that the reduction of ambient flow also depends on aquifer thickness. On a first order basis, the results for homogeneous aquifers may be used to estimate the behavior of a heterogeneous aquifer by computing a power-law average of the heterogeneous $K_h(z)$. Finally, it is evident from the analysis of vertical gradients on well water levels that in the presence of sufficiently high gradients ($\partial h/\partial z > 0.5$) it is physically possible for a well screen to be fully submerged below the water table, and yet have an internal water level below the top of the screen. Contrary to common perceptions, water levels in wells spanning the water table deviate significantly from the elevation of the formation water table when the local vertical gradient exceeds about 0.01.

Keywords: ambient flow; monitoring well; hydraulic head gradients; numerical simulation; well screens

1. Introduction

As documented in a recent study by Elci et al. (2001), measurable vertical flows in observation wells are to be expected in about 70% of long-screened wells. The flow is caused by the natural vertical hydraulic gradient that exists to some degree in virtually all aquifers. In the undisturbed natural system, such flows are normally small, but construction of an observation well produces a very high hydraulic conductivity pathway that allows for a non-negligible vertical flow in the wellbore, even if the head difference across a 10 m thick aquifer is only 0.5 cm (Elci et al., 2001). Such small head differences are difficult to even detect with careful measurement. However, an early warning concerning the danger of ignoring possible ambient flows in long-screened observation wells was issued by Reilly et al. (1989), and problems concerning a perceived bias in ground water samples collected from such wells was reported by Church and Granato (1996) and by Hutchins and Acree (2000). The more detailed hydraulic analysis presented by Elci et al. (2001) left little doubt that natural ambient flows will commonly make chemical concentration data collected from long-screened sampling wells unreliable and misleading. In a related study by Lacombe et al. (1995), the cross-contamination of aquifers through wellbores penetrating both formations and an intervening aquitard was demonstrated.

Illustrated in Figure 1 is the simulated effect of vertical ambient flow on a hypothetical contaminant plume in the vicinity of a fully-penetrating observation well at the U. S. Department of Energy Savannah River Site (Elci et al., 2001). Here, ambient flow in an observation well captures a simulated contaminant plume and transports the contaminant from the lower portion to the upper portion of the aquifer. This figure leaves little doubt concerning the potential importance of detecting and considering the effects of such flows on chemical concentration measurements.

Because of the small vertical head differences that are commonly involved, along with the recent development of highly sensitive borehole flowmeters, ambient flows are detected most readily by using such meters, commonly the heat-pulse or electromagnetic types (Morin et al., 1988; Molz and Young, 1993; Hutchins and Acree, 2000; Crisman et al., 2001). Given in Figure 2 is a summary of electromagnetic borehole flowmeter measurements that were obtained from a total of 142 monitoring wells at 16 sites across the USA. In 73% of the cases, a measurable amount of ambient flow was observed. The majority of the ambient flow cases, 62%, displayed a downward ambient flow, 31% of the cases displayed upward flow, and in 7% of the cases a mixed type of ambient flow (upward and downward) was observed (Elci et al., 2001). The range of measured ambient flow at all wells was 0.01 – 6.2 L/min.

Since natural ambient flows have now been shown to be ubiquitous, the question arises as to how one might control or minimize the effects of such potential flows. Two methods that immediately come to mind are to increase the vertical hydraulic resistance of fully-penetrating monitoring wells, such as by inserting flow obstructions, or to limit the screen length to less than full penetration. Elci et al. (2001) demonstrated that screen lengths less than 25% of the aquifer thickness, centered vertically about the midline of the aquifer, produce much less ambient flow relative to a fully-penetrating screen. Obviously, the problem can be solved by constructing cluster wells with extremely short screens, or using various types of multi-level sampling technology that is commercially available. These methodologies, however, are often relatively expensive, so the exploration of more economical alternatives may be justified. Providing such an exploration based on collected data and computer simulation is the first objective of the present study.

The detrimental effect of vertical head gradients would not be expected to be limited only to concentration measurements. Under more extreme conditions, one suspects that it is possible for natural vertical flows to raise or lower the water level in an observation well so that an erroneous hydraulic head measurement results. The formation of a seepage face at a pumped well in an unconfined aquifer is well known and continues to receive study (e.g. Taylor and Luthin, 1969; Neuman and Witherspoon, 1970; Shamsai and Narasimhan, 1991; Gefell et al., 1994; Kao et al., 2001). Because of the seepage face, the water level inside the well casing is not the same as the regional water table immediately adjacent to the well screen. However, to the authors' knowledge, the physical possibility that a seepage face can also form in an unpumped monitoring well placed in an aquifer with a vertical head gradient has not been subjected to detailed consideration. Therefore, a second objective is to present data and simulate the likely impact of relatively large vertical hydraulic gradients on water level measurements obtained in observation wells.

2. Analysis of the Effects of Increasing Wellbore Hydraulic Resistance and Screen Penetration

2.1 Methodology

To minimize the adverse effects of ambient wellbore flow, the wellbore hydraulic resistance can be increased (i.e. apparent hydraulic conductivity of wellbore can be decreased) or short screened, partially penetrating monitoring wells can be used. We analyzed the effects of these control measures on the magnitude of ambient flow by implementing a three-dimensional finite-difference ground water flow model in the vicinity of a monitoring well screened in a confined aquifer. The equation for steady-state ground water flow in a confined aquifer was solved with MODFLOW-96 (Harbaugh and McDonald, 1996):

$$\frac{\partial}{\partial x}\left(K_h \frac{\partial h}{\partial x}\right)+\frac{\partial}{\partial y}\left(K_h \frac{\partial h}{\partial y}\right)+\frac{\partial}{\partial z}\left(K_z \frac{\partial h}{\partial z}\right)=0 \quad (1)$$

where K_h is the horizontal hydraulic conductivity of the aquifer in the lateral flow directions, K_z is the vertical aquifer hydraulic conductivity, h is the hydraulic head, and x, y and z refer to spatial directions. The wellbore itself was represented as a narrow vertical zone of very high hydraulic conductivity, so the overall problem was modeled as flow in a heterogeneous aquifer, where the heterogeneity was the wellbore.

The numerical model domain consisted of 59 columns and rows, and 42 layers. The grid was irregularly spaced in the horizontal (Δx_{min} = 0.02 m, Δx_{max} = 0.22 m; Δy_{min} = 0.02 m; Δy_{max} = 0.22 m). Layers were regularly spaced with Δz=0.29 m. The boundary conditions and the general setup of the model are shown in Figure 3. More detailed information about the model properties were described in Elci et al. (2001).

In the present study, hydraulic head gradients were selected arbitrarily to be within the range of realistic field conditions, but different from those of Elci et al. (2001). The horizontal gradient was chosen as 1×10^{-4} and the vertical gradient, which has a more significant effect on ambient flow, was selected as 1×10^{-3}. The relationship between the (internal) wellbore resistance and the maximum ambient flow magnitude was determined by running a series of flow simulations for various selected wellbore hydraulic conductivities (K_w). The monitoring well inner diameter was 0.15 m and it was represented as a group of gridblocks that stretched from the top to the bottom of the model domain. The model grid was refined horizontally around the wellbore, which was positioned at the center of the model domain. The simulation of the wellbore was accomplished by assigning a much higher hydraulic conductivity to the gridblocks that represented the wellbore. The aquifer hydraulic conductivity was homogeneous and anisotropic (K_h/K_v=10). It was shown that ambient flow is very sensitive to K_h of the aquifer (Elci et al., 2001). Therefore, the series of simulations were run for different K_h values (0.5; 5.0 and 25 m/d).

Partial penetration of the well screen was expected to decrease the maximum ambient flow. The effects of partial penetration were systematically analyzed by executing the model for various screen lengths. Elci et al. (2001) changed the screen length about the midline of the aquifer and obtained a relationship between maximum ambient flow and screen penetration. This idea was further explored and shortened screens (50%, 25%, and 12.5% of total aquifer thickness) were positioned in the top and the bottom portion of the model domain to observe if ambient flow is related to the position of the screen. Furthermore, to determine the amount of reductions in maximum ambient flow due to the use of partially-penetrating well screens for various aquifer thicknesses, the above mentioned simulations were performed for ¼, ½, and 2 times the original aquifer thickness of 12.2 m. Simulations were performed on a homogeneous aquifer with a K_h=5.7 m/d, a value in the range of those measured in sediments at the Savannah River site.

In order to determine how heterogeneity might alter results from homogeneous aquifers, we executed the ambient flow model for a set of heterogeneous K_h data. Remaining model parameters and well properties remained unchanged from the preceding simulations. The K_h distribution of a monitoring well at the Savannah River Site measured with an electromagnetic flowmeter is presented in Figure 4. In order to provide some means for comparing simulations based on homogeneous and heterogeneous K_h distributions, the simulated maximum ambient flow in the well with the heterogeneous K_h data was compared to simulations with a power-averaged K_h derived from the heterogeneous distribution. The power average used is defined by Journel et al. (1986) as

$$\overline{K_h} = \left(\frac{1}{B} \int_0^B K_h{}^p (z) dz \right)^{1/p} \tag{2}$$

where *B* is aquifer thickness, and *z* is depth. By varying the exponent *p* between –1 and 1, the power average of K_h varies between the harmonic and the arithmetic averages, with the geometric mean corresponding to *p* approaching zero. Ambient flow simulations for a range of homogenous K_h, i.e. power-averaged K_h of the heterogeneous $K_h(z)$, were performed. Since the equivalent homogeneous K_h was expected to be close to the arithmetic average (*p*=1.0), K_h values calculated with *p* exponents of 1.0, 0.9, 0.8 and 0.7 were used in the simulations.

2.2 Results and Discussion

2.2.1 Effects of Increasing Wellbore Hydraulic Resistance

The effects of increasing the wellbore hydraulic resistance was determined by running a series of flow simulations for various selected wellbore hydraulic conductivities (K_w). K_w is inversely proportional to the wellbore hydraulic resistance. Simulation results showed that an increase of wellbore hydraulic resistance, i.e. decrease in K_w, caused a non-linear decrease in maximum ambient flow. Shown in Figure 5 are the relationships of simulated maximum ambient flow rates to decreasing K_w values for three different aquifer conductivities. It is evident from these observations that the necessary increase in wellbore hydraulic resistance to control ambient flow actually depends on the hydrogeological setting of the near-field aquifer. For example, lowering K_w has more impact, and is therefore more important, in aquifers with higher K_h (e.g.,

K_h=25 m/d) than in those having lower K_h (e.g., K_h=0.5 m/d). This is due to the fact that as one approaches a critical K_w, which decreases with decreasing K_h, the factor controlling total ambient flow through the wellbore is the quantity of ground water that can be supplied by the surrounding aquifer, not the increasing K_w. These critical K_w values were roughly estimated from Figure 5 as 3,250, 50,000 and 150,000 m/d for K_h values of 0.5, 5.0 and 25 m/d, respectively. Although critical values could change for head gradients of different magnitude, the general trend of increasing critical K_w with increasing aquifer K would remain intact.

For comparison, the apparent hydraulic conductivity for laminar flow in a well casing may be calculated as (McWhorter and Sunada, 1977):

$$K_w = \frac{{r_s}^2 \rho g}{8\mu} \qquad (3)$$

where ρ and μ are respectively the density and viscosity of ground water, r_s is the radius of the well screen, and g is the acceleration due to gravity. With property values that pertain to ground water at a temperature of 15°C, K_w was calculated as 5.2×10^5 m/d. This value is well above the previously mentioned critical K_w's, implying that long-screened monitoring wells in any hydrogeological setting with a typical vertical head gradient will be subject to ambient flow and its consequences, with the magnitude of the ambient flow limited only by the capability of the aquifer to supply water.

2.2.2 Systematic Analysis of Screen Penetration

Another measure to reduce ambient flow in monitoring wells is to use wells with partially penetrating screens. Shown in Figure 6 are the effects of shortening the well screens for a range of aquifer thickness. Here it was evident that the percent reduction of maximum ambient flow with the percent reduction of screen penetration also depends on the thickness of the aquifer. The effect of shortening the screen became more significant as the aquifer thickness decreased. For example, the ambient flow reduction with a screen penetrating 50% of the total aquifer thickness was 53, 60 and 73% for an aquifer thickness of 24.4, 12.2 and 6.1 m, respectively. The maximum ambient flowrate for any case in the 3.05 m thick aquifer was near negligible and would probably be not detected with an electromagnetic borehole flowmeter.

We could also confirm that the position of the well screen was not a factor in the occurrence of ambient flow in our homogeneous model domain. Therefore, maximum ambient flow for well screens positioned at the top, bottom, and about the center of the aquifer was essentially the same. Since the simulation was run for a homogeneous aquifer, the vertical head gradients were constant with depth. This position independency would not hold for a heterogeneous aquifer, where varying head gradients would occur in the vertical direction. Ambient flow magnitude would then depend on the manner in which permeable strata intersected the well screen.

2.2.3 First Order Application of Homogeneous Ambient Flow Results to Heterogeneous Aquifers

The arithmetic average (p=1) of the distribution $K_h(z)$ shown in Figure 4 was 0.426 m/d, and power averages for p values of 0.9, 0.8, and 0.7 were 0.393, 0.362, and 0.331, respectively. Shown in Figure 7 are simulated ambient flows for the heterogeneous K_h distribution and its power averages. Simulation results for both distributions agreed well with respect to the maximum ambient flow. A power-averaged K_h calculated with p=0.70~0.80 resulted in a simulated maximum ambient flow that was equivalent to its counterpart in the heterogeneous simulation. Therefore, our homogeneous simulations may be used to estimate ambient flows in heterogeneous aquifers using a power law average K_h with $p>0.7$.

3. Analysis of Steep Vertical Gradients on Water Levels in Wells

3.1 Seepage Faces in Unpumped Monitoring Wells

This analysis was motivated by subsurface characterization of low permeability unconsolidated sediments near the former R-reactor seepage basins located at the U.S. Department of Energy's Savannah River Site near Aiken, South Carolina. A total of 10 cone penetration tests (CPT) for volumetric soil moisture content were made near existing multi-level monitoring wells. Thus, water levels in the adjacent monitoring wells were available to compare with the probable water table elevations inferred from the CPT data. Two of the CPT moisture probe logs are shown in Figure 8. Close inspection of the CPT and well water level data revealed large differences between the top of the capillary fringe, determined by the CPT soil moisture probe, and the water level in the nearby well. At locations where the well screen spanned the top of the inferred capillary fringe, the difference was a meter or smaller (e.g. RR-4, Figure 8) and could be attributed to the estimated thickness of the capillary fringe (Freeze and Cherry, 1979). However, at other locations the top of the inferred capillary fringe lay above the well screen, and much larger differences where observed. The maximum difference was 4.5 m (RR-3 in Figure 8), which appeared unrealistically large, given the capillary-rise properties of the seepage basin soils, and led us to an analysis of the following possibility.

Illustrated in Figure 9 is a well screen submerged completely below the regional water table, but with a water level inside the casing that is located below the top of the screen, similar to the inferred field situation described previously. A hypothesized seepage face occurs over the entire portion of screen above the well water level, even though the well is not being pumped and the screen is completely submerged. Immediate questions were whether this situation is physically possible, and if so, under what conditions.

3.2 Methodology

To answer these questions, we first recalled that hydraulic head (*h*) is defined as the sum of pressure head (ψ) and elevation head (*z*):

$$h = \frac{p}{\rho g} + z = \psi + z \tag{4}$$

where both pressure and elevation are measured relative to arbitrary references. Common choices are atmospheric pressure ($p = \psi = 0$) and mean sea level ($z = 0$). Let z_{WT} denote the water table elevation and z_{WL} denote the water level inside the well casing, as shown in Figure 9. At both points the pressure is atmospheric, and so from definition (4):

$$h_{WT} = z_{WT} \tag{5}$$

$$h_{WL} = z_{WL} \tag{6}$$

Whether groundwater inside the screen is stagnant or flowing, any head difference across the water column inside the casing will be negligible for any practical well diameter, and

$$h_{Bot} = z_{WL} \tag{7}$$

at the bottom of the screen. Above the well water level, pressure is atmospheric and $h = z$ along the upper, unsaturated, portion of the screen. Starting from the well water level, head therefore increases linearly until at the top of the screen

$$h_{Top} = z_{Top} \tag{8}$$

From equations (6) through (8), hydraulic head along the well screen is seen to take on the variation plotted in Figure 9. Average head over the well screen becomes

$$\begin{aligned}\bar{h}_{Screen} &= \frac{(z_{Top}-z_{WL})\frac{1}{2}(h_{Top}+h_{WL})+(z_{WL}-z_{Bot})h_{WL}}{(z_{Top}-z_{Bot})} \\ &= \frac{(z_{Top}-z_{WL})\frac{1}{2}(z_{Top}+z_{WL})+(z_{WL}-z_{Bot})z_{WL}}{(z_{Top}-z_{Bot})}\end{aligned} \tag{9}$$

Now suppose a vertical head gradient exists ($\Delta h/\Delta z \neq 0$), due to recharge at the water table, and ambient flow occurs in the well. For simplicity, we can assume a constant and known gradient. Under these conditions, the head increases linearly with depth below the water table

$$\frac{h-h_{WT}}{z-z_{WT}} = \frac{\Delta h}{\Delta z} \tag{10}$$

Solving for head in terms of elevation, and considering equation (5), yields

$$h = \frac{\Delta h}{\Delta z}(z-z_{WT})+z_{WT} \tag{11}$$

Average formation head over the interval screened by the well, but under ambient flow conditions away from the well, is

$$\begin{aligned}\bar{h}_{Ambient} &= \frac{\Delta h}{\Delta z}\left[\frac{1}{2}(z_{Top}+z_{Bot})-z_{WT}\right]+z_{WT} \\ &= \frac{\Delta h}{\Delta z}\left[z_{Mid}-z_{WT}\right]+z_{WT}\end{aligned} \tag{12}$$

where z_{Mid} is the midpoint of the screen.

The presence of a well locally disturbs the head variation given by equation (10), by providing a hydraulic short-circuit; ground water enters an upper portion of the screen and exits along a lower portion. However, because the well is not pumped, inflows and outflows cancel and the well represents neither a source nor sink from a far field perspective. For practical purposes, the average head in the formation is unaffected by the well. Therefore, equations (9) and (12) can be equated. The result, after some algebraic manipulations, was a quadratic equation for well water level (z_{WL})

$$z_{WL}^2 - 2z_{Bot} z_{WL} + z_{Top}^2 - 2\overline{h}_{Ambient}(z_{Top} - z_{Bot}) = 0 \tag{13}$$

with solution

$$\begin{aligned} z_{WL} &= \frac{-b + \sqrt{b^2 - 4ac}}{2a} \\ a &= 1 \\ b &= -2z_{Bot} \\ c &= z_{Top}^2 - 2\overline{h}_{Ambient}(z_{Top} - z_{Bot}) \end{aligned} \tag{14}$$

$$z_{WL} = z_{Bot} + \{(z_{Top} - z_{Bot})[(z_{WT} - z_{Top}) + (z_{WT} - z_{Bot})](1 - \Delta h / \Delta z)\}^{1/2}$$

Of course, numerical values computed from equation (14) and inputs must satisfy the assumptions of this pseudo-static analysis, namely, $z_{WT} \geq z_{Top}$ and $z_{Top} \geq z_{WL} \geq z_{Bot}$. The solution given by equation (14) can be written more concisely in terms of depths below the water table as

$$d_{WL} = d_{Bot} - \left[\left(d_{Bot}^2 - d_{Top}^2\right)(1 - \Delta h / \Delta z)\right]^{1/2} \tag{15}$$

where $d_{Top} \equiv z_{WT} - z_{Top}$, $d_{Bot} \equiv z_{WT} - z_{Bot}$ and the constraints become $0 \leq d_{Top} \leq d_{WL} \leq d_{Bot}$.

Returning to the questions first posed in the preceding section, example applications of equation (14) were considered (Table 1). The examples involved a 3 m well screen set 1.5 m below the water table at 10 m elevation, and ambient vertical head gradients of 0.51 and 0.75. A vertical gradient greater than 0.50 was required to achieve the conditions depicted in Figure 9 according to solution (14). The gradient of 0.75 was midway between the lower threshold, and the maximum gradient of 1.0 for water table field conditions.

In order to confirm the results of the example calculations, the conditions specified in Table 1 were simulated in detail numerically for an isotropic, homogeneous porous medium using Richards equation. The purpose of the numerical simulation is to account for saturated/unsaturated flow phenomena not considered in the preceding pseudo-static analysis. The model simulations were performed on a three-dimensional Cartesian grid using the FACT code (Hamm and Aleman, 2000) and brick-shaped finite-elements. The model domain size was 44×44×12 m and 32×32×60 elements. The mesh extended vertically from 3 m above the water table and 4.5 m above the well screen top, to 4.5 m below the bottom of the screen. From top down, the vertical mesh was comprised of 5 finite-elements at 0.6 m thickness, 10 at 0.15 m, 30 at 0.1 m, 10 at 0.15 m, and 5 at 0.6 m thickness. A vertical hydraulic gradient of 0.51 (0.75) was achieved by setting the surface infiltration rate to 0.51 (0.75) times the saturated hydraulic conductivity (K) of the formation, which was arbitrary. The specific value chosen was K = 0.00147 m/d (isotropic). The horizontal hydraulic gradient was set to zero. The well diameter was chosen as 0.10 m. Extending from the centerline of the well outward, elements in the horizontal plane were dimensioned: 0.05, 0.025, 0.035, 0.055, 0.075, 0.125, 0.175, 0.28, 0.43, 0.65, 1, 1.4, 2.2, 3.2, 4.9 and 7.4 m. The well was approximated in the model by the four elements in the horizontal plane touching the well centerline. Over the 3 m screen section, the saturated conductivity of this column of elements was set to 10,000 times the saturated aquifer conductivity. The effect of the impermeable casing above the screen was simulated by setting saturated conductivity 10,000 times smaller than aquifer K. Water retention and relative permeability curves for the entire mesh were defined by Van Genuchten (1980) functional forms using the parameter settings for "Clay" from Schaap and Leij (1998, Table 4). For these settings, the slope of the relative permeability curve was infinite at saturation. To avoid inherent numerical difficulties with this situation, the Van Genuchten curve was subsequently modified by using linear interpolation between saturations of 0.99 and 1 to keep the slope finite. Sensitivity studies were conducted using a wide-range of alternative soil characteristic curves for the aquifer, well screen and well casing regions, in various combinations. Provided the saturated K contrasts between the aquifer and well segments were sufficiently large, the predicted well water level was found to be rather insensitive to the choice of soil characteristic curves in each of these regions, so the unsaturated portion of the flow regime was apparently not important to the bottom-line result.

3.3 Results and Discussion

Results for the example calculations are summarized in Table 1. For a hydraulic gradient of 0.51, the well water level was predicted from equation (14) to fall slightly below the top of the screen. Because the seepage face was of negligible thickness, the well water level (z_{WL}) was the same as the screen-average head ($h_{screen} = h_{ambient}$), but 1.53 m below the formation water table. For a vertical head gradient of 0.75, the well water level computed from equation (14) was 7.62 m, which lay 0.88 m below the top of the screen. The well level was 0.13 m lower than the average head along the screen and 2.38 m below the formation water table. The corresponding numerical simulations agreed with the calculations in Table 1 in that the water level within the well was at an elevation of 8.49 and 7.67 m for vertical head gradients of 0.51 and 0.75, respectively (Figure 10). Evidently, the quasi-static analysis is quite good for these types of problems.

The basic mechanism for the head difference was that the formation head at the screen midpoint under undisturbed conditions was below the top of the screen, due to the sufficiently steep downward gradient. A second mechanism was that the well acted again as a "short circuit". Since head was lower at the bottom of the formation, ground water was seen to flow into the well along the upper portion of the screen, and leave over the lower portion. Inflow occurs along the seepage face and for some distance below the well water level. Although the well lowered the local water table slightly (Figure 10), that perturbation was small compared to the discrepancy between the water table and well water level.

This example demonstrates that the conditions depicted schematically in Figure 9 are possible for realistic parameter values, and can result in differences of a few meters between the water table and well water level. Therefore, a well with a water level within the screen zone does not necessarily measure the water table elevation. Equation (14) or (15) can be used to explore the range of conditions required for the situation shown in Figure 9 to occur. For example, the threshold gradient for the conditions of Figure 9 to occur is defined by setting $d_{WL} = d_{Top}$ in equation (15):

$$\frac{\Delta h}{\Delta z} = \frac{d_{WL}}{d_{WL} + (d_{Bot} - d_{Top})/2} \qquad (16)$$

Further information is presented in Figure 11, which identifies a range of hydraulic gradients yielding a water level below the screen top for a screen length of 3 m and various depths below the water table. Note that in general a steep vertical head gradient is required for the conditions of Figure 9 to occur. In addition, the well screen must be positioned within a certain depth range below the water table. For typical gradients (e.g. $\Delta h / \Delta z < 0.1$), the effect is negligible, if present at all.

4. Conclusions and Recommendations

This paper presented further analyses of ambient flow in monitoring wells and their impacts on ground water monitoring. Control of ambient flow for a long-screened, fully-penetrating monitoring well is possible by increasing the vertical hydraulic resistance. As our modeling results indicated, the necessary increase in wellbore hydraulic resistance depends on the hydrogeological setting of the near-field aquifer. For example, for $\partial h/\partial z=1\times10^{-3}$ and K_h=0.5 m/d, the hydraulic conductivity of the wellbore K_w had to be decreased at least to a critical value of 3,250 m/d to reduce the magnitude of occurring ambient flow. As K_h increased, lowering K_w (increasing wellbore hydraulic resistance) had more impact on the reduction of ambient flow.

Shorter well screen lengths as opposed to fully-penetrating, long well screens resulted in lower ambient flow rates, as it was also pointed out in Elci et al. (2001). However, the effect of shortening the screen became more significant as the thickness of the aquifer decreased. We observed from the simulation results that for $\partial h/\partial z=1\times10^{-3}$ any screen length in a 3 m thick aquifer experienced near negligible ambient flow. Furthermore, it was confirmed that ambient flow occurrence in a relatively homogeneous aquifer was independent of the vertical screen position. The power-law average of $K_h(z)$ for a heterogeneous aquifer, with $p>0.7$, may be used in homogenous ambient flow simulations to estimate ambient flows in that aquifer. Generally speaking, ambient flow simulation results based on the range of head gradients and aquifer hydraulic conductivities tested in this paper and Elci et al.(2001), can give an idea about the magnitude of ambient flow. When a significant amount of ambient flow is expected, adverse effects on ground water sampling will occur.

The analysis of well water levels implied the following general conclusions of importance to water level monitoring. It is physically possible for a well screen to be fully submerged below the water table, and yet have an internal water level below the top of the screen. This possibility was demonstrated by a pseudo-static algebraic analysis and a more rigorous numerical simulation. Therefore, a water level below the top of screen does not necessarily mean the screen spans the water table, contrary to conventional interpretation. If this possibility occurs, the internal well water level is not even equal to head in the formation averaged over the screened interval. For typical monitoring well screens (e.g. 3 to 7 m in length), relatively steep downward gradients ($\partial h/\partial z > 0.5$) are required for a significant discrepancy of water levels to occur. However, this condition can also be observed for lesser gradients coupled with sufficiently long well screens. The occurrence of this effect may not be that rare in practice, and would be important to water level interpretation where it does occur.

The agreement between the pseudo-static analysis and the more rigorous numerical simulation was excellent for both gradients. This indicates that the simple pseudo-static analysis can be used for data interpretation, and that there is no need to resort to a numerical model in practice.

References

Church, P.E., Granato, G.E. 1996. Bias in ground-water data caused by well-bore flow in long-screen wells. Ground Water 34(2), 262-273.

Crisman, S.A., Molz, F.J., Dunn, D.L., Sappington, F.C. 2001. Application procedures for the electromagnetic borehole flowmeter in shallow unconfined aquifers. Ground Water Monitoring & Remediation 21(4), 96-100.

Elci, A., Molz, F.J., Waldrop, W.R. 2001. Implications of observed and simulated ambient flow in monitoring wells. Ground Water 39(6), 853-862.

Freeze, R.A., Cherry, J.A. 1979. Groundwater. Prentice-Hall, Englewood Cliffs, New Jersey.

Gefell, M.J., Thomas, G.M., Rossello, S.J. 1994. Maximum water-table drawdown at a fully-penetrating pumping well. Ground Water 32(3), 411-419.

Hamm, L.L., Aleman, S.E. 2000. FACT (Version 2.0) Subsurface Flow and Contaminant Transport Documentation and User’s Guide. Westinghouse Savannah River Company Technical Report WSRC-TR-99-00282, Rev.0.

Harbaugh, A.W., McDonald, M.G. 1996. User's documentation for MODFLOW-96, an update to the U.S. Geological Survey modular finite-difference ground-water flow model: U.S. Geological Survey Open-File Report 96-485, 56 p.

Hutchins, S.R., Acree, S.D. 2000. Ground water sampling bias observed in shallow, conventional wells. Ground Water Monitoring & Remediation 20(1), 86-93.

Journel, A.G., Deutsch, C., Desbarats, A.J. 1986. Power averaging for block effective permeability. Society of Petroleum Engineers 15128.

Kao, C., Bouarfa, S., Zimmer, D. 2001. Steady state analysis of unsaturated flow above a shallow water-table aquifer drained by ditches. Journal of Hydrology 250(1-4), 122-133.

Lacombe, S., Sudicky, E.A., Frape, S.K., Unger, A.J.A. 1995. Influence of leaky boreholes on cross-formational groundwater flow and contaminant transport. Water Resources Research 31(8), 1871-1882.

McWhorter, D.B., Sunada, D.K. 1977. Ground-water hydrology and hydraulics. Water Resources Publications, Fort Collins, Colorado.

Molz, F.J., Young, S.C. 1993. Development and application of borehole flowmeters for environmental assessment. The Log Analyst, 13-23.

Morin, R.H., Hess, A.E., Paillet, F.L. 1988. Determining the distribution of hydraulic conductivity in a fractured limestone aquifer by simultaneous injection and geophysical logging. Ground Water 26(5), 587-595.

Neuman, S.P., Witherspoon, P.A. 1970, Finite element method of analyzing steady seepage with a free surface. Water Resources Research 6, 889-897.

Reilly, T.E., Franke, L., Bennett, G.D. 1989. Bias in groundwater samples caused by wellbore flow. Journal of Hydraulic Eng. 115(2), 270-276.

Schaap, M.G., Leij, F.J. 1998. Database-related accuracy and uncertainty of pedotransfer functions. Soil Science 163(10), 765-779.

Shamsai, A., Narasimhan, T.N. 1991. A numerical investigation of free surface-seepage face relationship under steady state flow conditions. Water Resources Research 27, 409-421.

Taylor, G.S., Luthin, J.N. 1969. Computer methods for transient analysis of water table aquifers. Water Resources Research 5, 144-152.

Van Genuchten, M.Th. 1980. A closed-form equation for predicting the hydraulic conductivity of unsaturated soils. Soil Sci. Am. J. 44, 892-898.

Figure 1: Simulated tracer plume in an aquifer with a monitoring well subject to ambient flow. Iso-surface shows 0.1 mg/L of tracer concentration. (adapted from Elci et al., 2001)

Figure 2: Summary of ambient flow measurements with the electromagnetic borehole flowmeter.

Figure 3: Boundary conditions of ambient flow model. (Elci et al, 2001)

Figure 4: Hydraulic conductivity distribution by flowmeter analysis for a monitoring well at the Savannah River Site.

Figure 5: Change of ambient flow magnitude for various selected wellbore hydraulic conductivities (K_w). Head gradients in the surrounding aquifer are $\partial h/\partial x = \partial h/\partial y = 1\times10^{-4}$ and $\partial h/\partial z = 1\times10^{-3}$.

Figure 6: Effect of partially penetrating screens on the maximum ambient flow rate for different aquifer thicknesses. Head gradients are $\partial h/\partial x = \partial h/\partial y = 4.7\times10^{-3}$ and $\partial h/\partial z = 5\times10^{-3}$.

Figure 7: Comparison of simulated ambient flow for a heterogeneous K distribution and its various power averages.

Figure 8: Cone Penetration Testing (CPT) data from pushes near two clustered water level monitoring wells. The dotted box depicts length of the well screen. (DU = well water level; WT + CF = water table + capillary fringe)

Figure 9 Hydraulic head profile associated with a well with an internal seepage face.

Figure 10: Numerical simulation of a monitoring well subject to ambient flow using parameters given in Table 1. Dashed contour lines indicate hydraulic head.

Figure 11: Change of d_{WL} as a function of vertical head gradient for various d_{Top}.

Figure 1

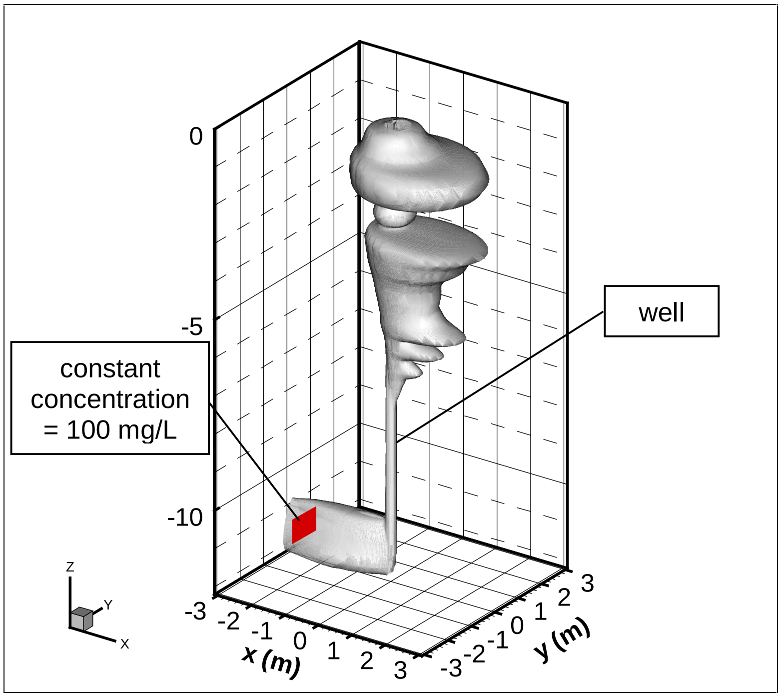

well
constant
concentration
= 100 mg/L
0
-5
-10
-3 -2 -1 0 1 2 3
x (m)
-3 -2 -1 0 1 2 3
y (m)
Z
Y
X

Figure 2

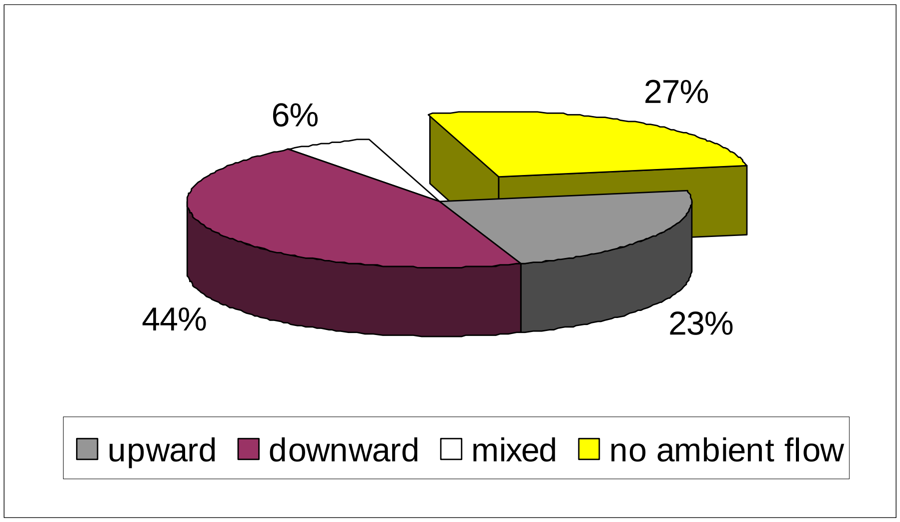

Figure 3

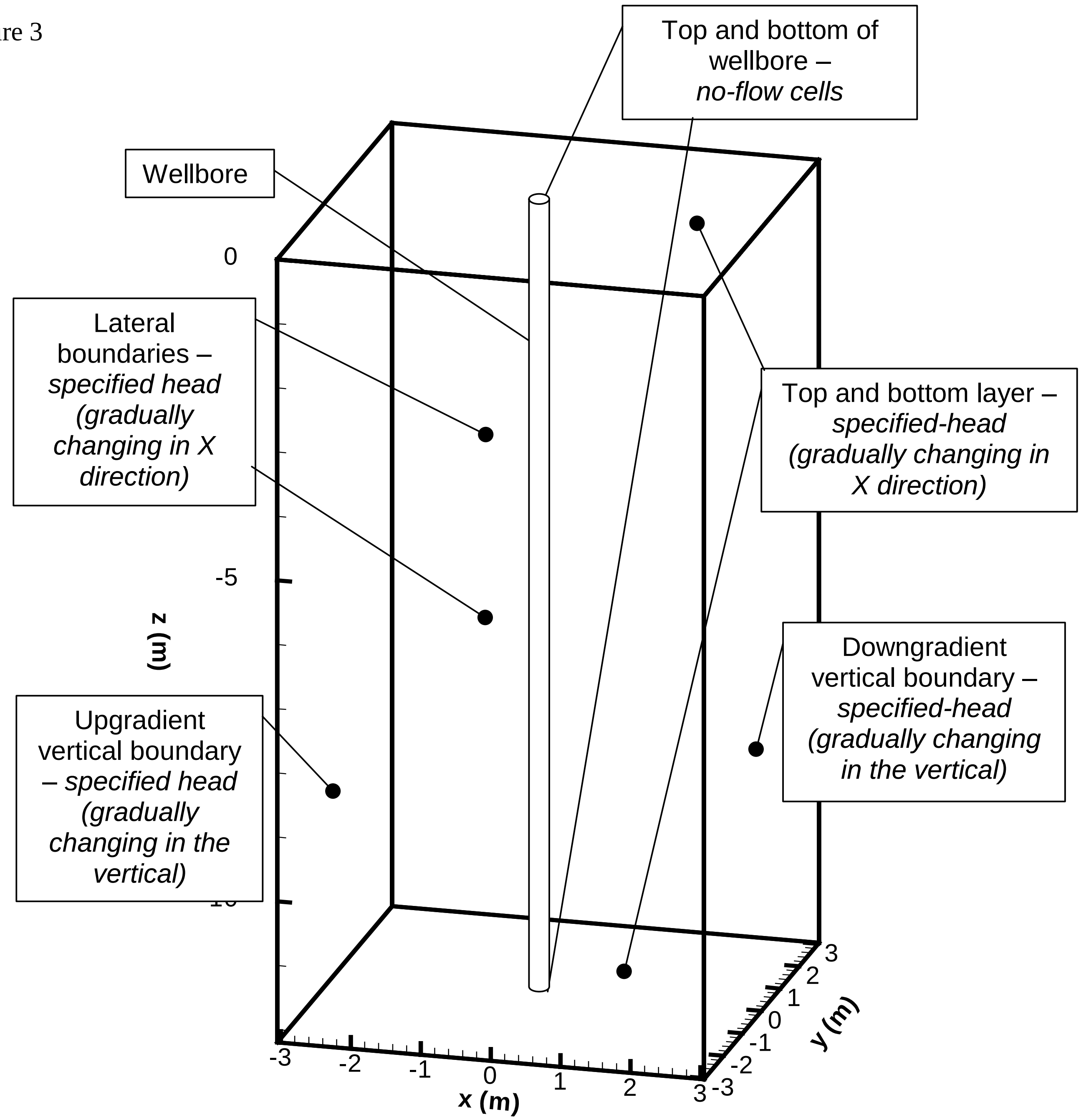
Top and bottom of wellbore – *no-flow cells*
Wellbore
Lateral boundaries – *specified head (gradually changing in X direction)*
Top and bottom layer – *specified-head (gradually changing in X direction)*
Downgradient vertical boundary – *specified-head (gradually changing in the vertical)*
Upgradient vertical boundary – *specified head (gradually changing in the vertical)*
0
-5
z (m)
-3
-2
-1
0
1
2
3
x (m)
-3
-2
-1
0
1
2
3
y (m)

Figure 4

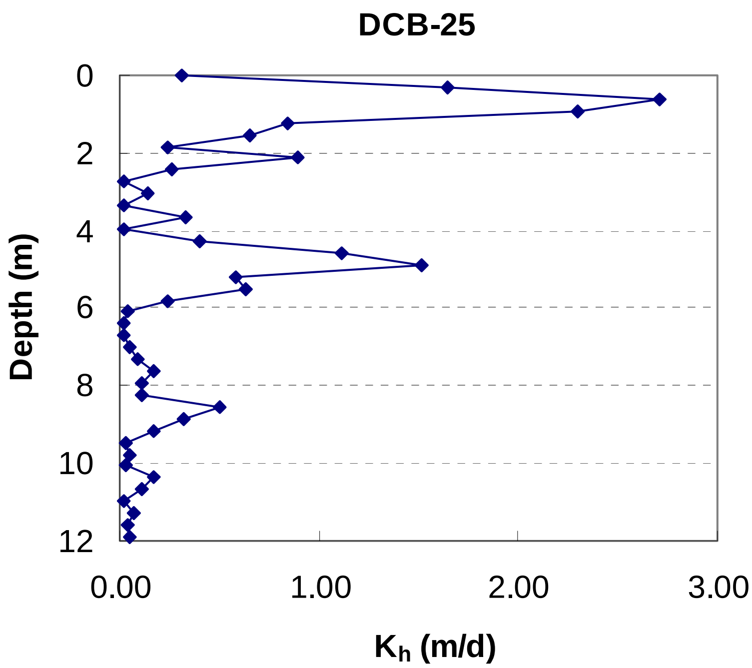

Figure 6

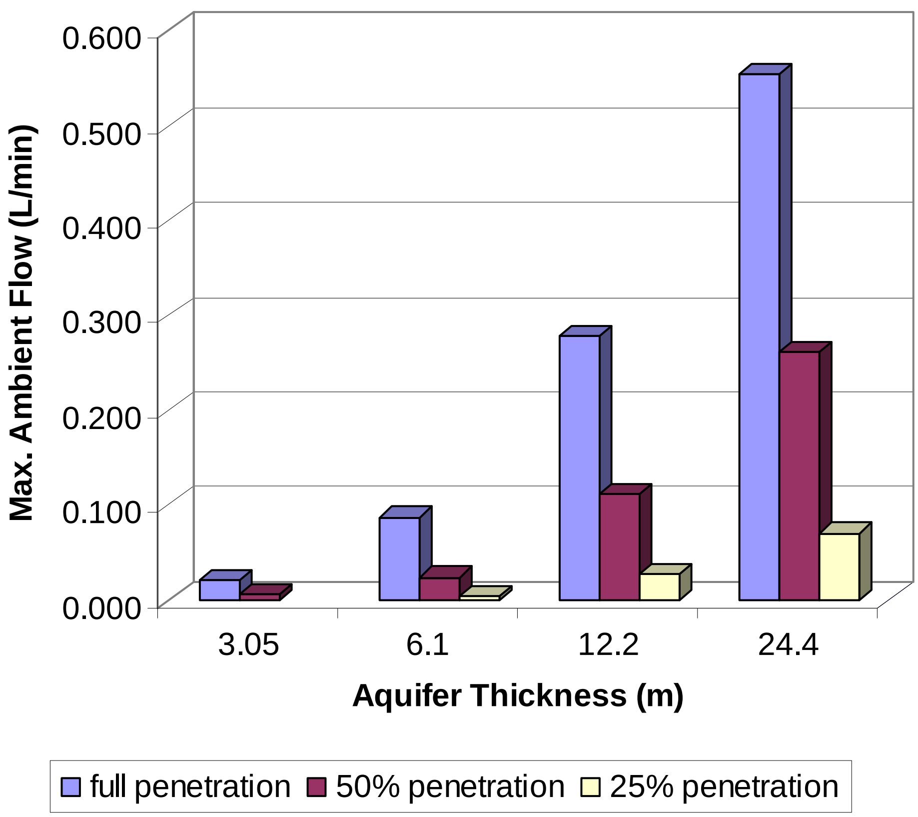
0.600
0.500
0.400
0.300
0.200
0.100
0.000
Max. Ambient Flow (L/min)
3.05
6.1
12.2
24.4
Aquifer Thickness (m)
full penetration
50% penetration
25% penetration

Figure 5

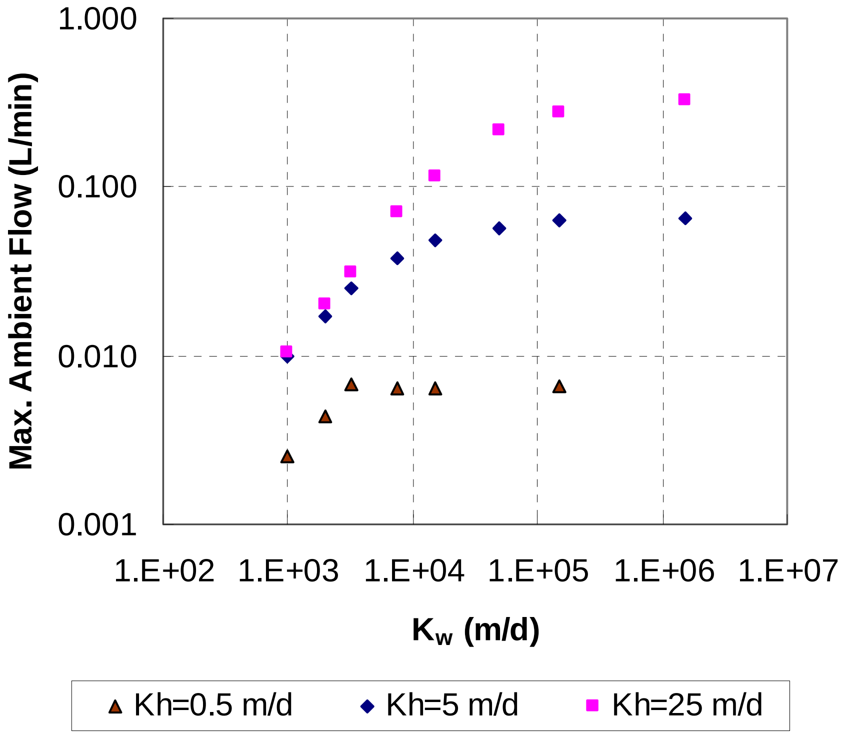
1.000
0.100
0.010
0.001
Max. Ambient Flow (L/min)
1.E+02
1.E+03
1.E+04
1.E+05
1.E+06
1.E+07
K_w (m/d)
Kh=0.5 m/d
Kh=5 m/d
Kh=25 m/d

Figure 7

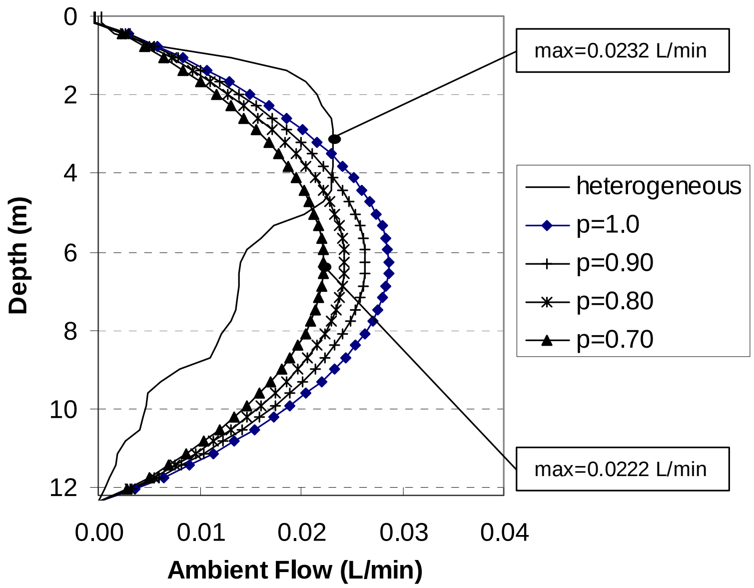

max=0.0232 L/min
max=0.0222 L/min
heterogeneous
p=1.0
p=0.90
p=0.80
p=0.70
Depth (m)
0
2
4
6
8
10
12
0.00
0.01
0.02
0.03
0.04
Ambient Flow (L/min)

Figure 8

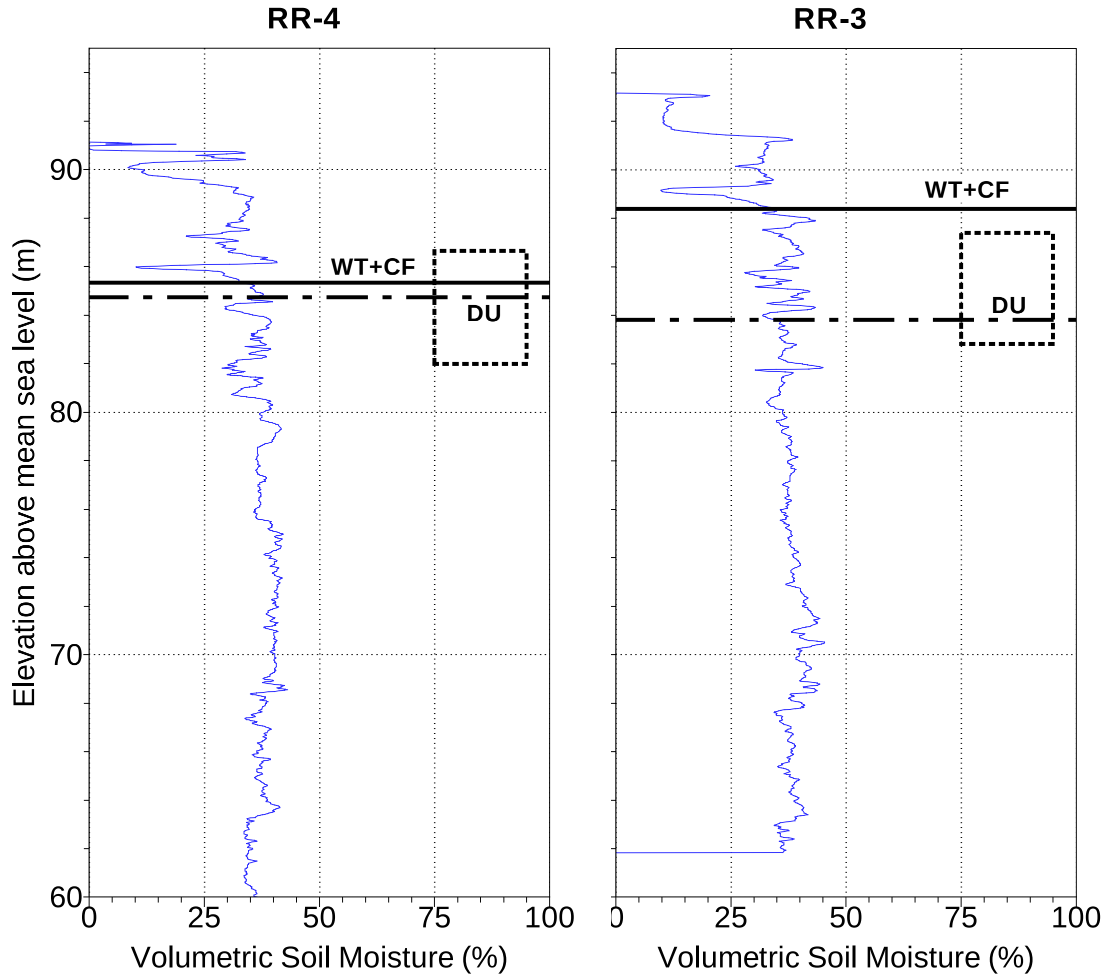
RR-4
RR-3
Elevation above mean sea level (m)
90
80
70
60
WT+CF
DU
0
25
50
75
100
Volumetric Soil Moisture (%)

Figure 9

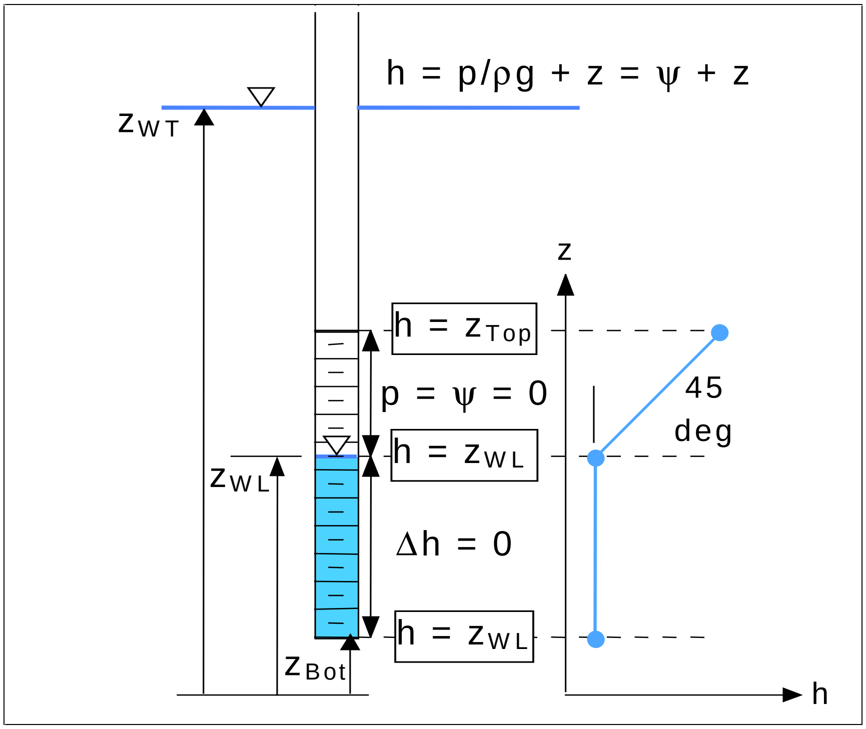

Figure 10

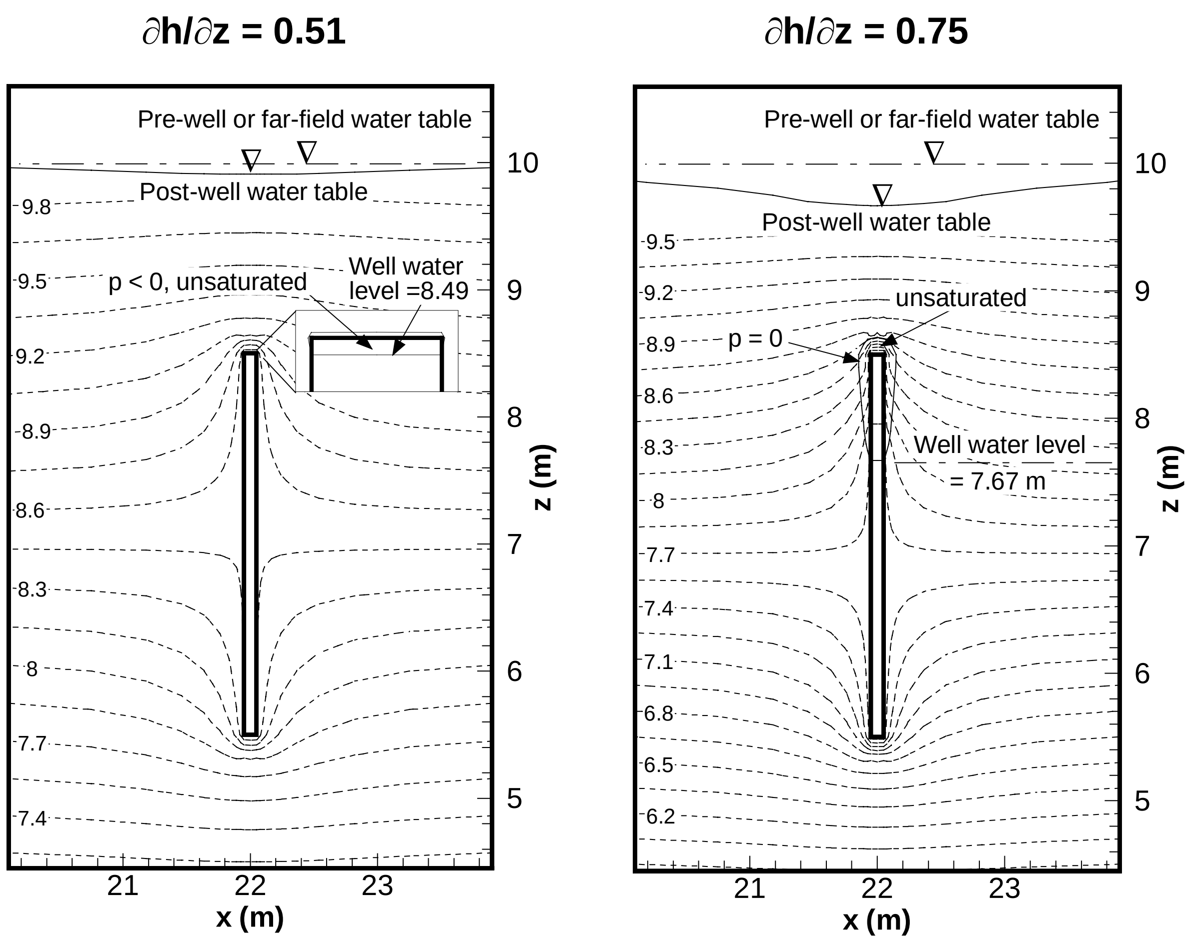
∂h/∂z = 0.51
Pre-well or far-field water table
Post-well water table
p < 0, unsaturated
Well water
level =8.49
9.8
9.5
9.2
8.9
8.6
8.3
8
7.7
7.4
10
9
8
7
6
5
z (m)
21
22
23
x (m)
∂h/∂z = 0.75
Pre-well or far-field water table
Post-well water table
unsaturated
p = 0
Well water level
= 7.67 m
9.5
9.2
8.9
8.6
8.3
8
7.7
7.4
7.1
6.8
6.5
6.2
10
9
8
7
6
5
z (m)
21
22
23
x (m)

Figure 11

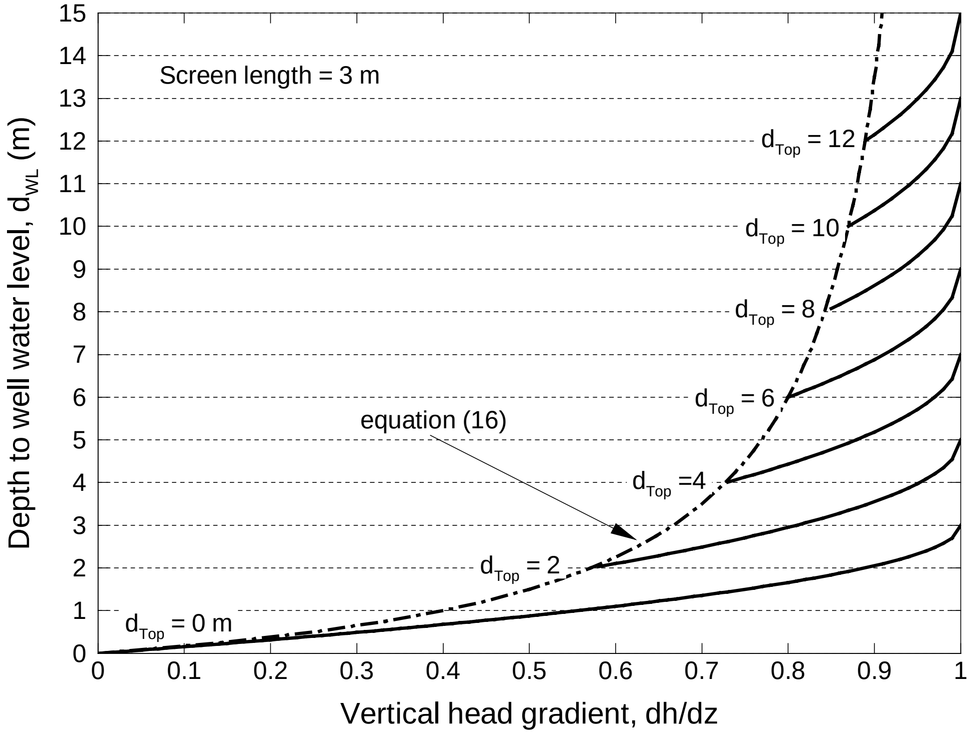

Screen length = 3 m
equation (16)
d_{Top} = 0 m
d_{Top} = 2
d_{Top} =4
d_{Top} = 6
d_{Top} = 8
d_{Top} = 10
d_{Top} = 12
Depth to well water level, d_{WL} (m)
Vertical head gradient, dh/dz
0 0.1 0.2 0.3 0.4 0.5 0.6 0.7 0.8 0.9 1
0 1 2 3 4 5 6 7 8 9 10 11 12 13 14 15

Table 1: Example of a submerged well screen with well water beneath the screen top (internal seepage face).

		Example 1	Example 2
Given conditions	Water table elevation, z_{WT} (m)	10.0	10.0
	Screen top elevation (m)	8.5	8.5
	Screen bottom elevation (m)	5.5	5.5
	Vertical head gradient $\partial h/\partial z$	0.51	0.75
Results	$h_{ambient}$ (m)	8.47	7.75
	h_{screen} (m)	8.47	7.75
	Well Water Level, z_{WL} (m)	8.47	7.62
	$h_{screen} - z_{WL}$ (m)	0	0.13
	$z_{WT} - z_{WL}$ (m)	1.53	2.38